A new HLLCEP Riemann solver with both elactic and plastic waves for 1D elastic-plastic flows with multi-materials

Li Liu[1],Junbo Cheng [1,*]

January 10, 2019

[1] Institute of Applied Physics and Computational Mathematics, Beijing 100094, China

Abstract

A new HLLC-type approximate Riemann solver is constructed with both the structures of elastic and plastic waves for 1D multi-material elastic-plastic flows with the hypo-elastic constitutive model and the von Mises yield criterion. The new method takes a detail consideration of the plastic waves to get a correct relation in the star regions between the contact wave or multi-material interface. Combining with third-order WENO scheme and third-order Runge-Kutta scheme, a high-order cell-centered Lagrangian scheme for 1D elastic-plastic flows is used in this paper. A number of numerical expriments are carried out. Showed by the numerical results, due to the rationable consideration of the plastic waves, the most attractive advantage of the new HLLCEP solver is the accurate resolution of the interface between different materials in the elastic-plastic flows.

HLLC Riemann solver with elastic and plastic waves, high-order cell-centered Lagrangian scheme, WENO scheme, hypo-elastic constitutive model, elastic-plastic flows

1 Introduction

In this paper, a new HLLC-type approximate Riemann solver is developed, with the capibility of resolving both elactic and plastic waves, to simulate one-dimensional multi-material elastic-plactic solid problems with the isotropic elastic-plastic model [1] and von Mises' yielding condition in the framework of high-order cell-centered Lagrangian scheme.

Many elastic-plastic solid problems of interest involve large deformations and are treated as flows. Up till now, elastic-plastic flows can be mainly simulated in three ways, Eulerian method [2, 3, 4], staggered Lagrangian schemes [1] and cell-centered Lagrangian schemes [5, 6, 7, 8] which is considered in this paper. Cell-centered Lagrangian scheme is derived based on the Godunov method and has combined many advantages from both staggered Lagrangian schemes and Eulerian methods. Firstly, it's no need to use artificial viscosity which must be used in the staggered Lagrangian schemes, besides, it's can also be used in both hyper-elastic models and hypo-elastic models [5, 6, 7, 8] as a Lagrangian scheme.

In the Godunov type method approach, a core process is to construct the conservative flux by solving the solution of a Remainn problem at each cell face. As the Remiann problem contains many physical structures especially in elastic-plastic flows, such as elastic waves, plastic waves and contact waves or interfaces between different materials, the property of the approximate Remainn solver may do a magnitude influence in the simulation. Recently, there is a lot of works have been done in this area. For example, Gavrilyuk et al. [9] analyzed the structure of Riemann solution to construct a Riemann solver for the linear elastic system of hyperbolic non-conservative models for transverse waves, wherein an extra evolution equation was added in order to make the elastic transformations reversible in the absence of shock waves. Despres [10] built a shock solution to a non-conservations reverisible system of hypo-elasticity models and found that a sonic point is necessary to construct compression solution that begins at a constrained comressed state. Cheng eta al. [11] analyzed the wave structures of one-dimensional elastic-plastic flows and developed an effective two-rarefaction Riemann solver with elastic waves (TRRSE) and build the second-order and third-order cell-centered Lagrangian schemes based on the TRRSE, but the TRRSE is a little expensive as iteration method

is used in it. In [12], for one-dimensional elastic-plastic flows, Cheng introduced a HLLCE Riemann solver, which is fast and efficient in resolving elastic waves and plastic waves for numerical examples in [12], but Cheng evaluated the deviatoric stresses from the following assumption: a pressure is continuous across the contact wave in the Rieman solver. This assumption is valid for pure fluids, but for elastic-plastic flows, this assumption maybe lead to some errors. There are three cases we need to consider.

1. If both states in the star regions near the contact wave are elastic, this assumption does not results in errors;
2. If the both states reach the elastic limit, there are two cases we need take into account:
   (a) if the both materials across the interface are same, this assumption does not results in errors, too;
   (b) if the both materials are different, this assumption will results in big errors because the yielding strengths of different materials are always different;
3. If one state in one side of the interface are yielded, but another does not, this assumption also results in big errors.

For the above consideration, in this paper, we aim to construct a new HLLC-type Riemann solver for 1D elastic-plastic flows, in the new solver, both the elastic waves and plastic waves are resolved and the assumption in [12] that the pressure is continuous across the interface is deleted, correspondingly, the errors introduced by the assumption will also be eliminated.

Combined with an improved third-order WENO scheme[13] and Runge-Kutta scheme, a high-order cell-centered Lagrangian scheme is given in this paper for one-dimensional elastic-plastic flows with multi-materials.

This paper is organized as follows. In section 2, we briefly introduce the goverining equations to be studied. In section 3, the HLLEP method is constructed. Then, high-order cell-centered Lagrangian schemes for a non-conservative system of elastic plasticity is given in section 4, some numerical examples are presented to validate the method. Conclusions are shown in section 5.

2 Governing equations

The equations for a continuous one-dimensional solid in differential form given as

$$\partial_t \mathbf{U} + \partial_x \boldsymbol{F}(\mathbf{U}) = 0,\ x \in\ \Omega \subset \mathbf{R},\ t > 0,$$

where

$$\mathbf{U} = \begin{bmatrix} \rho \\ \rho u \\ \rho E \end{bmatrix}, \quad \mathbf{F} = \begin{bmatrix} \rho u \\ \rho u^2 - \sigma_x \\ (\rho E - \sigma_x) u \end{bmatrix}, \tag{2.1}$$

ρ, u, σ_x and E are the density, velocity in $x-$direction, Cauchy stress and total energy per unit volume, respectively, E has the relation with specific internal energy e as

$$E = e + \frac{1}{2}u^2, \tag{2.2}$$

$$\sigma_x = -p + s_{xx}, \tag{2.3}$$

where p and s_{xx} denote hydrostatic pressure and deviatoric stress in the $x-$ direction, respectively.

In this paper, the elastic energy is not included in the total energy. The exclution of the elastic energy is usual for practical engineering problems [7] and is different from that in Ref.[9].

The relation of the pressure with the density and the specific internal energy is gotten from the equation of state (EOS). In this paper, we consider the Mie-Grüneisen EOS,

$$p(\rho, e) = \rho_0 a_0^2 f(\eta) + \rho_0 \Gamma_0 e, \tag{2.4}$$

where $f(\eta) = \frac{(\eta-1)(\eta-\Gamma_0(\eta-1)/2)}{(\eta-s(\eta-1))^2}$, $\eta = \frac{\rho}{\rho_0}$, ρ_0, a_0, s, and Γ_0 are constant parameters of the Mie-Grüneisen EOS.

Hooke's law is used here to describe the relationship between the deviatoric stress and the strain,

$$\dot{s}_{xx} = 2\mu\left(\dot{\varepsilon}_x - \frac{1}{3}\frac{\dot{V}}{V}\right), \tag{2.5}$$

where μ is the shear modulus, V is the volume, and the dot means the material time derivative,

$$\dot{()} = \frac{\partial()}{\partial t} + u\frac{\partial()}{\partial t}, \tag{2.6}$$

and

$$\dot{\varepsilon}_x = \frac{\partial u}{\partial x}, \quad \frac{\dot{V}}{V} = \frac{\partial u}{\partial x}. \tag{2.7}$$

Using Eq.(2.7), Eq.(2.5) can be rewritten as

$$\frac{\partial s_{xx}}{\partial t} + u\frac{\partial s_{xx}}{\partial t} = \frac{4}{3}\mu\frac{\partial u}{\partial x}. \tag{2.8}$$

The Von Mises' yileding condition is used here to describe the elastic limit. In one spatial dimension, the von Mises' yielding criterion is given by

$$|s_{xx}| \leq \frac{2}{3}Y_0, \tag{2.9}$$

where Y_0 is the yield strength of the material in simple tension.

3 HLLCEP

3.1 The Riemann problem

The Riemann problem for the 1D time dependent elastic-plastic equations is given as follows:

$$\begin{cases} \partial_t\rho + \partial_x(\rho u) = 0, \\ \partial_t(\rho u) + \partial_x(\rho u^2 + p - s_{xx}) = 0, \\ \partial_t(\rho E) + \partial_x\left[(\rho E + p - s_{xx})u\right] = 0, \\ \partial_t s_{xx} + u\partial_x s_{xx} - \frac{4}{3}\partial_x u = 0, \\ Q(x, t=0) = \begin{cases} Q_L, \text{ if } x < 0, \\ Q_R, \text{ if } x \geq 0, \end{cases} \end{cases} \tag{3.1}$$

where $Q = (\rho, \rho u, \rho E, s_{xx})^T$.

3.2 Jacobian matrix

For the Mie-Grüneisen EOS, the problem (3.1) can be written as

$$\partial_t \boldsymbol{Q} + \boldsymbol{J}(\boldsymbol{Q})\partial_x \boldsymbol{Q} = 0, \tag{3.2}$$

where

$$J = \begin{bmatrix} 0 & 1 & 0 & 0 \\ -u^2 + \frac{\partial p}{\partial \rho} + \Gamma(\frac{u^2}{2} - e) & u(2-\Gamma) & \Gamma & -1 \\ (\Gamma(\frac{u^2}{2} - e) - e + \frac{\sigma_x}{\rho} + \frac{\partial p}{\partial \rho})u & -\Gamma u^2 - \frac{\sigma_x}{\rho} + e & (1+\Gamma)u & -u \\ \frac{4}{3}\mu\frac{u}{\rho} & -\frac{4}{3}\mu\frac{1}{\rho} & 0 & u \end{bmatrix}, \tag{3.3}$$

where $\Gamma = \frac{\Gamma_0\rho_0}{\rho}$.

The eigenvalues of the coefficient matrix $\boldsymbol{J}(\boldsymbol{Q})$ are given as

$$\lambda_1 = \lambda_2 = u, \quad \lambda_3 = u - c, \quad \lambda_4 = u + c, \tag{3.4}$$

where

$$\begin{cases} c = \sqrt{a^2 - \dfrac{\rho_0}{\rho^2}\Gamma_0 s_{xx} + \dfrac{4}{3}\dfrac{\mu}{\rho}}, \\ a^2 = \dfrac{\partial p}{\partial \rho} + \dfrac{p}{\rho^2}\dfrac{\partial p}{\partial e} = a_0^2 \dfrac{\partial f}{\partial \eta} + \dfrac{p}{\rho^2}\rho_0\Gamma_0. \end{cases} \tag{3.5}$$

The corresponding right eigenvectors are

$$r_1 = \begin{bmatrix} \frac{1}{b_1} \\ \frac{u}{b_1} \\ 0 \\ 1 \end{bmatrix}, \quad r_2 = \begin{bmatrix} -\frac{\Gamma}{b_1} \\ -\frac{\Gamma u}{b_1} \\ 1 \\ 0 \end{bmatrix}, \quad r_3 = \frac{1}{\phi^2}\begin{bmatrix} 1 \\ u - c \\ h - uc \\ \phi^2 \end{bmatrix}, \quad r_4 = \frac{1}{\phi^2}\begin{bmatrix} 1 \\ u + c \\ h + uc \\ \phi^2 \end{bmatrix}, \tag{3.6}$$

where

$$b_1 = \frac{\partial p}{\partial \rho} - \Gamma E, \quad h = E + \frac{p - s_{xx}}{\rho}, \tag{3.7}$$

and

$$\phi^2 = a^2 - \frac{\rho_0}{\rho^2}\Gamma_0 s_{xx} - c^2 = -\frac{4\mu}{3}\frac{1}{\rho}. \tag{3.8}$$

3.3 States between the contact wave or the interface

For a system without molercular diffusion, there is no materials convecting cross the contact wave or interface, so the velocities between the discontinuity are always equal, $u_L^* = u_R^*$. This can also be verified by the eigenvectors in Eq.(3.6).

Using the eigenvectors in Eq.(3.6), for the λ_1-wave we have

$$\frac{d\rho}{\frac{1}{b_1}} = \frac{d\rho u}{\frac{u}{b_1}} = \frac{d\rho E}{0} = \frac{ds_{xx}}{1}. \tag{3.9}$$

From the above equations, we can easily deduce that

$$du = 0, \quad d(s_{xx} - p) = 0, \tag{3.10}$$

which means

$$u_L^* = u_R^*, \tag{3.11}$$

and

$$\sigma_{x,L}^* = \sigma_{x,R}^*, \tag{3.12}$$

where $()_L^*$ and $()_R^*$ denote $()$ in the region of $\mathbf{W}_L^*$ and $\mathbf{W}_R^*$, respectively. Here we do not show the details of the derivation for simplicity of presentation.

Using the eigenvectors (3.6), for the λ_2-wave we have

$$\frac{d\rho}{\frac{-\Gamma}{b_1}} = \frac{d\rho u}{\frac{-u\Gamma}{b_1}} = \frac{d\rho E}{1} = \frac{ds_{xx}}{0}. \tag{3.13}$$

From the above equations, we can easily deduce that

$$du = 0, \quad dp = 0, \quad ds_{xx} = 0, \tag{3.14}$$

which means

$$u_L^* = u_R^*, \tag{3.15}$$

$$p_L^* = p_R^*, \quad s_{xx,L}^* = s_{xx,R}^*, \tag{3.16}$$

where $()^*_L$ and $()^*_R$ denote () in the region of $\mathbf{W}^*_L$ and $\mathbf{W}^*_R$, respectively.

From Eq.(3.16), we get that

$$\sigma^*_{x,L} = \sigma^*_{x,R}. \tag{3.17}$$

At last, for the λ_1 and λ_2 waves, one can find that the following two equations always hold:

$$u^*_L = u^*_R, \quad \sigma^*_{x,L} = \sigma^*_{x,R}. \tag{3.18}$$

Using the Rankine-Hugoniot relations between the contact wave or the interface

$$\boldsymbol{F}^*_R = \boldsymbol{F}^*_L + s^*(\boldsymbol{U}^*_R - \boldsymbol{U}^*_L). \tag{3.19}$$

From the first and second components of the above system, one can get

$$\rho^*_R u^*_R = \rho^*_L u^*_L + s^*(\rho^*_R - \rho^*_L), \tag{3.20}$$

$$\rho^*_R u^{*2}_R - \sigma^*_R = \rho^*_L u^{*2}_L - \sigma^*_L + s^*(\rho^*_R u^*_R - \rho^*_L u^*_L). \tag{3.21}$$

Generally, for convenience,

$$s^* = u^*_L = u^*_R. \tag{3.22}$$

3.4 A relation between ρ and s_{xx} in 1D elastic-plastic equation system

Thanks to (2.6), from the 1D elastic-plastic equations in Eq.(3.1), the equations of the density and the deviatoric stress can be written as

$$\frac{\partial u}{\partial x} = -\frac{1}{\rho}\frac{d\rho}{dt}, \tag{3.23}$$

and

$$\frac{ds_{xx}}{dt} = \frac{4}{3}\mu\frac{\partial u}{\partial x}. \tag{3.24}$$

Substituting (3.23) into (3.24) yields

$$\frac{ds_{xx}}{dt} = -\frac{4}{3}\mu\frac{1}{\rho}\frac{d\rho}{dt}. \tag{3.25}$$

Take an integration,

$$s_{xx1} = -\frac{4}{3}\mu\ln(\frac{\rho_1}{\rho_0}) + s_{xx0}. \tag{3.26}$$

The subscript 1 and 0 mean the states in front of and behind a wave. This relation always holds if there is no yielding in the integration path.

3.5 The constructing details of HLLCEP method

Now we considered the constructing details of HLLCEP method. As there possible exist left-going or right-going plastic waves, there may be three to five waves in the results of the Riemann problem, that depends on the yielding state on the left side and right side.

3.5.1 Pre-evaluating the states without considering of plastic waves

At first we do not know the yielding states, so assume that there is no plastic wave in and the material is totally yielding or totally not yielding, we consider the structures of Fig.1. If the result contains yielding process, we will turn the case into one in Fig.2-4.

The HLLC is given as follows,

$$\boldsymbol{U}^{\text{HLLCEP}}_{\text{Case1}}(x,t) = \begin{cases} \boldsymbol{U}_L, & \text{if} \quad \dfrac{x}{t} \le s_L, \\ \boldsymbol{U}^*_L, & \text{if} \quad s_L \le \dfrac{x}{t} \le s^*, \\ \boldsymbol{U}^*_R, & \text{if} \quad s^* \le \dfrac{x}{t} \le s_R, \\ \boldsymbol{U}_R, & \text{if} \quad \dfrac{x}{t} \ge s_R, \end{cases} \tag{3.27}$$

and the corresponding Eulerian numerical flux and Lagrangian numerical flux are

$$\boldsymbol{F}^{\text{Euler}}_{\text{Case1}}(x,t) = \begin{cases} \boldsymbol{F}_L, & \text{if} \quad \dfrac{x}{t} \le s_L, \\ \boldsymbol{F}^*_L, & \text{if} \quad s_L \le \dfrac{x}{t} \le s^*, \\ \boldsymbol{F}^*_R, & \text{if} \quad s^* \le \dfrac{x}{t} \le s_R, \\ \boldsymbol{F}_R, & \text{if} \quad \dfrac{x}{t} \ge s_R, \end{cases} \tag{3.28}$$

$$\boldsymbol{F}^{\text{Lag}}_{\text{Case1}}(x,t) = \begin{cases} \boldsymbol{f}^*_L, & \text{if} \quad s_* \ge \dfrac{x}{t}, \\ \boldsymbol{f}^*_R, & \text{if} \quad s^* \le \dfrac{x}{t}. \end{cases} \tag{3.29}$$

According to the Rankine-Hugoniot conditions between left elastic wave,

$$\boldsymbol{F}^*_L = \boldsymbol{F}_L + s_L(\boldsymbol{U}^*_L - \boldsymbol{U}_L), \tag{3.30}$$

we can get

$$\rho^*_L u^*_L = \rho_L u_L + s_L(\rho^*_L - \rho_L), \tag{3.31}$$

and

$$\rho^*_L u^{*2}_R - \sigma^*_L = \rho_L u^2_L - \sigma_L + s_L(\rho^*_L u^*_L - \rho_L u_L). \tag{3.32}$$

Using the relation of $u^*_L = u^*_R = s^*$ in Eq.(3.22), the speed of contact wave can be evaluated as

$$\hat{s}^* = \frac{\sigma_L - \sigma_R + \rho_L u_L(s_L - u_L) - \rho_R u_R(s_R - u_R)}{\rho_L(s_L - u_L) - \rho_R(s_R - u_R)}, \tag{3.33}$$

the density is solved as

$$\hat{\rho}^*_L = \frac{\rho_L(u_L - s_L)}{\hat{s}^* - s_L}. \tag{3.34}$$

Samilar, we can get the density on the right as

$$\hat{\rho}^*_R = \frac{\rho_R(u_R - s_R)}{\hat{s}^* - s_R}. \tag{3.35}$$

where the speeds of left and right elastic waves are evaluted as

$$s_L = \min(u_L - c_L, u_R - c_R), \quad s_R = \max(u_L + c_L, u_R + c_R). \tag{3.36}$$

Based on the assumption above, as there is no plastic wave in, we can take the relation of Eq.(3.26), and the deviatoric stress is evaluated as

$$\hat{s}^*_{xxL} = -\frac{4}{3}\mu \ln(\frac{\hat{\rho}^*_L}{\rho_L}) + s_{xxL}, \quad \hat{s}^*_{xxR} = -\frac{4}{3}\mu \ln(\frac{\hat{\rho}^*_R}{\rho_R}) + s_{xxR}. \tag{3.37}$$

Using the pre-evaluated values of $\hat{s}^*_{xxL}$ and $\hat{s}^*_{xxR}$, we can classify the true condtion into the following four cases.

3.5.2 Case 1: No plastic wave

In this case, If $|s_{xxL}| < \frac{2}{3}Y_0$ and $|\hat{s}^*_{xxL}| < \frac{2}{3}Y_0$, all the states on the left are not yielding. Or $|s_{xxL}| \ge \frac{2}{3}Y_0$ and $|\hat{s}^*_{xxL}| \ge \frac{2}{3}Y_0$, all the states on the left are yielding. The assumption holds on the left. Meanwhile, if $|s_{xxR}| < \frac{2}{3}Y_0$ and $|\hat{s}^*_{xxR}| < \frac{2}{3}Y_0$, Or $|s_{xxR}| \ge \frac{2}{3}Y_0$ and $|\hat{s}^*_{xxR}| \ge \frac{2}{3}Y_0$, the assumption holds on the right. Then the structures truely are the case in Fig.1.

Then

$$s^* = \hat{s}^*, \quad \rho^*_L = \hat{\rho}^*_L, \quad \rho^*_R = \hat{\rho}^*_R, \tag{3.38}$$

$$s^*_{xxL} = \Upsilon(\hat{s}^*_{xxL}), \quad s^*_{xxR} = \Upsilon(\hat{s}^*_{xxR}) \tag{3.39}$$

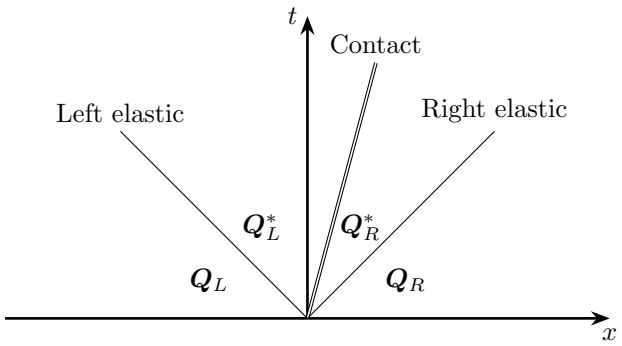

Figure 1: The structures of HLLCEP method, case 1: without plastic wave.

where,

$$\Upsilon(\omega) = \begin{cases} \omega, \text{ if } |\omega| \leq \dfrac{2}{3}Y_0, \\ \dfrac{2}{3}Y_0, \text{ if } \omega > \dfrac{2}{3}Y_0, \\ -\dfrac{2}{3}Y_0, \text{ if } \omega < -\dfrac{2}{3}Y_0. \end{cases} \tag{3.40}$$

The Cauchy stresses are solved by Eq.(3.32),

$$\sigma_L^* = \sigma_R^* = \sigma_L - \rho_L(s_L - u_L)(s^* - u_L).$$

Then we can get the pressure by $p = s_{xx} - \sigma$.

$$p_L^* = s_{xxL}^* - \sigma_L^*, \; p_R^* = s_{xxR}^* - \sigma_R^*. \tag{3.41}$$

3.5.3 Case 2: with only the left plastic wave

If $|s_{xxL}| \leq \frac{2}{3}Y_0 \leq |\hat{s}_{xxL}^*|$, there exists a plastic wave on the left as showed in Fig.2. We need to solve the state of $\widetilde{\boldsymbol{Q}}_L$. The HLLCEP is given as follows in this case,

$$\boldsymbol{U}_{\text{Case2}}^{\text{HLLCEP}}(x,t) = \begin{cases} \boldsymbol{U}_L, & \text{if } \dfrac{x}{t} \leq \widetilde{s}_L, \\ \widetilde{\boldsymbol{U}}_L, & \text{if } \widetilde{s}_L \leq \dfrac{x}{t} \leq s_L, \\ \boldsymbol{U}_L^*, & \text{if } s_L \leq \dfrac{x}{t} \leq s^*, \\ \boldsymbol{U}_R^*, & \text{if } s^* \leq \dfrac{x}{t} \leq s_R, \\ \boldsymbol{U}_R, & \text{if } \dfrac{x}{t} \geq s_R, \end{cases} \tag{3.42}$$

and the corresonding Eulerian and Lagrangian numerical flux are

$$\boldsymbol{F}_{\text{Case2}}^{\text{Euler}}(x,t) = \begin{cases} \boldsymbol{F}_L, & \text{if } \dfrac{x}{t} \leq \widetilde{s}_L, \\ \widetilde{\boldsymbol{F}}_L, & \text{if } \widetilde{s}_L \leq \dfrac{x}{t} \leq s_L, \\ \boldsymbol{F}_L^*, & \text{if } s_L \leq \dfrac{x}{t} \leq s^*, \\ \boldsymbol{F}_R^*, & \text{if } s^* \leq \dfrac{x}{t} \leq s_R, \\ \boldsymbol{F}_R, & \text{if } \dfrac{x}{t} \geq s_R, \end{cases} \tag{3.43}$$

$$\boldsymbol{F}^{\text{Lag}}_{\text{Case2}}(x,t) = \begin{cases} \boldsymbol{f}^*_L, & \text{if} \quad s_* \geq \dfrac{x}{t}, \\ \boldsymbol{f}^*_R, & \text{if} \quad s^* \leq \dfrac{x}{t}. \end{cases} \tag{3.44}$$

Using the Rankine-Hugoniot relation of the left plastic wave,

$$\widetilde{\rho}_L(\widetilde{u}_L - \widetilde{s}_L) = \rho_L(u_L - \widetilde{s}_L), \tag{3.45}$$
$$\widetilde{\rho}\widetilde{u}_L(\widetilde{u}_L - \widetilde{s}_L) = \rho_L u_L(u_L - \widetilde{s}_L) + \widetilde{\sigma}_L - \sigma_L, \tag{3.46}$$
$$\widetilde{\rho}\widetilde{E}_L(\widetilde{u}_L - \widetilde{s}_L) = \rho_L E_L(u_L - \widetilde{s}_L) + \widetilde{\sigma}_L\widetilde{u}_L - \sigma_L u_L, \tag{3.47}$$

where yielding happened behind the plastic wave, so the deviatoric stress and density are taken as

$$\widetilde{s}_{xxL} = \begin{cases} -\dfrac{2}{3}Y_0, & \text{if} \quad \rho^*_L > \rho_L, \\ \dfrac{2}{3}Y_0, & \text{if} \quad \rho^*_L < \rho_L, \end{cases} \tag{3.48}$$

and

$$\widetilde{\rho}_L = \begin{cases} \rho_L \text{exp}\left(\dfrac{Y_0}{2\mu} + \dfrac{3s_{xxL}}{4\mu}\right) & \text{if} \quad \rho^*_L > \rho_L, \\ \rho_L \text{exp}\left(-\dfrac{Y_0}{2\mu} + \dfrac{3s_{xxL}}{4\mu}\right) & \text{if} \quad \rho^*_L < \rho_L. \end{cases} \tag{3.49}$$

The unknowns are the wave speed $\widetilde{s}_L$, the velocity $\widetilde{u}_L$, the pressure $\widetilde{p}_L$ and the specific internal energy $\widetilde{E}_L$. In the following, we will give the derivations of them.

From Eq.(3.45) we can get the wave speed as

$$\widetilde{s}_L = \frac{\widetilde{\rho}_L\widetilde{u}_L - \rho_L u_L}{\widetilde{\rho}_L - \rho_L}, \tag{3.50}$$

and have the relation of

$$u_L - \widetilde{s}_L = \frac{(u_L - \widetilde{u}_L)\widetilde{\rho}_L}{\widetilde{\rho}_L - \rho_L}. \tag{3.51}$$

Substituting Eq.(3.45) into Eq.(3.46), we have

$$\rho_L(\widetilde{u}_L - u_L)(u_L - \widetilde{s}_L) = \widetilde{\sigma}_L - \sigma_L, \tag{3.52}$$

then substituting Eq.(3.51) into it, we can get the following relation

$$-t(\widetilde{u}_L - u_L)^2 = \widetilde{\sigma}_L - \sigma_L, \tag{3.53}$$

where

$$t = \frac{\rho_L\widetilde{\rho}_L}{\widetilde{\rho}_L - \rho_L}. \tag{3.54}$$

Similar to Eq.(3.52), Eq.(3.46) can be changed into

$$t(u_L - \widetilde{u}_L)(\widetilde{E}_L - E_L) = \widetilde{\sigma}_L\widetilde{u}_L - \sigma_L u_L, \tag{3.55}$$

and we also know that $E = e + \frac{1}{2}u^2$, then we have

$$\widetilde{e}_L - e_L = -\frac{\sigma_L + \widetilde{\sigma}_L}{2t}. \tag{3.56}$$

The EOS (2.4) can be written as

$$e = c_0 p - c_1 f(\rho/\rho_0), \tag{3.57}$$

where $c_0 = \frac{1}{\rho_0\Gamma_0}$ and $c_1 = \frac{a_0^2}{\Gamma_0}$.

Substituting (3.57) and $\sigma = -p + s_{xx}$ into (3.56), we can get the pressure behind the plastic wave as

$$\widetilde{p}_L = \frac{2t(c_1 f(\widetilde{\rho}_L) + e_L) - (\sigma_L + \widetilde{s}_{xxL})}{2tc_0 - 1}, \tag{3.58}$$

and the Cauchy stress is solved by $\widetilde{\sigma}_L = -\widetilde{p}_L + \widetilde{s}_{xxL}$. Using Eq.(3.53) we can get

$$(\widetilde{u}_L - u_L)^2 = \frac{\sigma_L - \widetilde{\sigma}_L}{t}, \tag{3.59}$$

then the velocity is solved,

$$\widetilde{\boldsymbol{u}}_L = \begin{cases} u_L + \sqrt{\dfrac{\sigma_L - \widetilde{\sigma}_L}{t}} & \text{if } \rho_R^* > \rho_R, \\ u_L - \sqrt{\dfrac{\sigma_L - \widetilde{\sigma}_L}{t}} & \text{if } \rho_R^* < \rho_R. \end{cases} \tag{3.60}$$

After solving the state of $\widetilde{\boldsymbol{Q}}_L$, using a samilar process with Section 3.5.2, the states of $\boldsymbol{Q}_L^*$ and $\boldsymbol{Q}_R^*$ can be solved out as follows.

The contace wave speed is

$$s^* = \frac{\widetilde{\sigma}_L - \sigma_R + \widetilde{\rho}_L \widetilde{u}_L (s_L - \widetilde{u}_L) - \rho_R u_R (s_R - u_R)}{\widetilde{\rho}_L (s_L - \widetilde{u}_L) - \rho_R (s_R - u_R)}, \tag{3.61}$$

The densities are

$$\rho_L^* = \frac{\widetilde{\rho}_L (\widetilde{u}_L - s_L)}{s^* - s_L}, \quad \rho_R^* = \frac{\rho_R (u_R - s_R)}{s^* - s_R}, \tag{3.62}$$

where the left and right elastic wave speeds are evaluted as

$$s_L = \min(\widetilde{u}_L - \widetilde{c}_L, u_R - c_R), \quad s_R = \max(\widetilde{u}_L + \widetilde{c}_L, u_R + c_R). \tag{3.63}$$

The deviatoric stresses are evaluated as

$$\overline{s}_{xxL}^* = -\frac{4}{3}\mu \ln(\frac{\rho_L^*}{\rho_L}) + s_{xxL}, \ \ \overline{s}_{xxR}^* = -\frac{4}{3}\mu \ln(\frac{\rho_R^*}{\rho_R}) + s_{xxR}, \tag{3.64}$$

then using von Mises' yielding condition

$$s_{xxL}^* = \Upsilon(\overline{s}_{xxL}^*), \quad s_{xxR}^* = \Upsilon(\overline{s}_{xxR}^*). \tag{3.65}$$

The Cauchy stresses are given as

$$\sigma_L^* = \sigma_R^* = \widetilde{\sigma}_L - \widetilde{\rho}_L (s_L - \widetilde{u}_L)(s^* - \widetilde{u}_L), \tag{3.66}$$

and the pressures are

$$p_L^* = s_{xxL}^* - \sigma_L^*, \quad p_R^* = s_{xxR}^* - \sigma_R^*. \tag{3.67}$$

3.5.4 Case 3: with only the right plastic wave

If $|s_{xxR}| \le \frac{2}{3} Y_0 \le |\hat{s}_{xxR}^*|$, there exists a plastic wave on the right as showed in Fig.3. We need to solve the state of $\widetilde{\boldsymbol{Q}}_R$ at first. The HLLCEP is given in this case as,

$$\boldsymbol{U}_{\text{Case3}}^{\text{HLLCEP}}(x,t) = \begin{cases} \boldsymbol{U}_L, & \text{if } \ \dfrac{x}{t} \le s_L, \\ \boldsymbol{U}_L^*, & \text{if } \ s_L \le \dfrac{x}{t} \le s^*, \\ \boldsymbol{U}_R^*, & \text{if } \ s^* \le \dfrac{x}{t} \le s_R, \\ \widetilde{\boldsymbol{U}}_R, & \text{if } \ s_R \le \dfrac{x}{t} \le \widetilde{s}_R, \\ \boldsymbol{U}_R, & \text{if } \ \dfrac{x}{t} \ge \widetilde{s}_R, \end{cases} \tag{3.68}$$

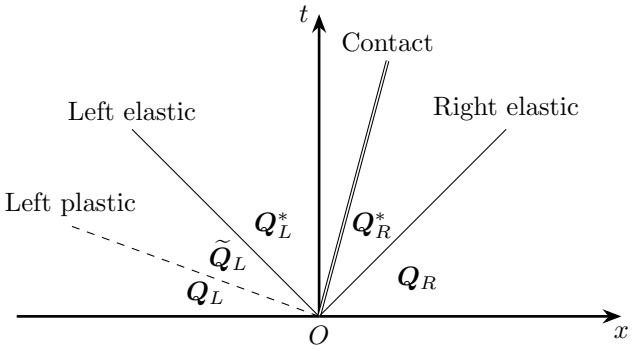

Figure 2: The structures of HLLCEP method, case 2: with only the left plastic wave.

and the corresonding Eulerian and Lagrangian numerical flux are

$$\boldsymbol{F}^{\text{Euler}}_{\text{Case3}}(x,t) = \begin{cases} \boldsymbol{F}_L, & \text{if} \quad \dfrac{x}{t} \le s_L, \\ \boldsymbol{F}^*_L, & \text{if} \quad s_L \le \dfrac{x}{t} \le s^*, \\ \boldsymbol{F}^*_R, & \text{if} \quad s^* \le \dfrac{x}{t} \le s_R, \\ \widetilde{\boldsymbol{F}}_R, & \text{if} \quad s_R \le \dfrac{x}{t} \le \widetilde{s}_R, \\ \boldsymbol{F}_R, & \text{if} \quad \dfrac{x}{t} \ge \widetilde{s}_R, \end{cases} \tag{3.69}$$

$$\boldsymbol{F}^{\text{Lag}}_{\text{Case3}}(x,t) = \begin{cases} \boldsymbol{f}^*_L, & \text{if} \quad s_* \ge \dfrac{x}{t}, \\ \boldsymbol{f}^*_R, & \text{if} \quad s^* \le \dfrac{x}{t}. \end{cases} \tag{3.70}$$

The deviatoric stress, density and pressure are given as

$$\widetilde{s}_{xxR} = \begin{cases} -\dfrac{2}{3}Y_0, & \text{if} \quad \rho^*_R > \rho_R, \\ \dfrac{2}{3}Y_0, & \text{if} \quad \rho^*_R < \rho_R, \end{cases} \quad \widetilde{\rho}_R = \begin{cases} \rho_R \text{exp}\left(\dfrac{Y_0}{2\mu} + \dfrac{3s_{xxR}}{4\mu}\right) & \text{if} \quad \rho^*_R > \rho_R, \\ \rho_R \text{exp}\left(-\dfrac{Y_0}{2\mu} + \dfrac{3s_{xxR}}{4\mu}\right) & \text{if} \quad \rho^*_R < \rho_R, \end{cases} \tag{3.71}$$

$$\widetilde{p}_R = \frac{2t(c_1 f(\widetilde{\rho}_R) + e_R) - (\sigma_R + \widetilde{s}_{xxR})}{2tc_0 - 1}, \quad t = \frac{\rho_R \widetilde{\rho}_R}{\widetilde{\rho}_R - \rho_R}, \tag{3.72}$$

where $c_0 = \frac{1}{\rho_0 \Gamma_0}$ and $c_1 = \frac{a_0^2}{\Gamma_0}$. The Cauchy stress and velocity are

$$\widetilde{\sigma}_R = -\widetilde{p}_R + \widetilde{s}_{xxR}, \tag{3.73}$$

$$\widetilde{u}_R = \begin{cases} u_R + \sqrt{\dfrac{\sigma_R - \widetilde{\sigma}_R}{t}} & \text{if} \ \ \rho^*_R > \rho_R, \\ u_R - \sqrt{\dfrac{\sigma_R - \widetilde{\sigma}_R}{t}} & \text{if} \ \ \rho^*_R < \rho_R. \end{cases} \tag{3.74}$$

After solving the state of $\widetilde{\boldsymbol{Q}}_R$, we can solve the states of $\boldsymbol{Q}^*_L$ and $\boldsymbol{Q}^*_R$.
The contact wave speed is

$$s^* = \frac{\sigma_L - \widetilde{\sigma}_R + \rho_L u_L(s_L - u_L) - \widetilde{\rho}_R \widetilde{u}_R(s_R - \widetilde{u}_R)}{\rho_L(s_L - u_L) - \widetilde{\rho}_R(s_R - \widetilde{u}_R)}. \tag{3.75}$$

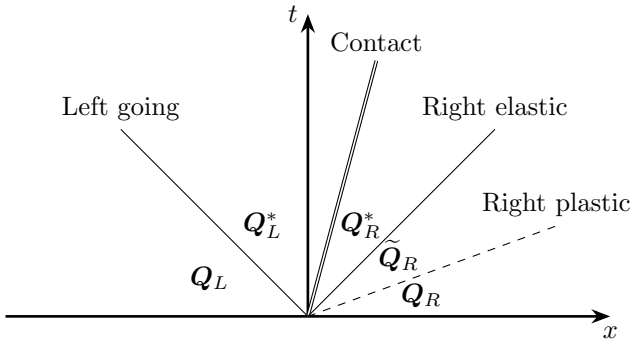

Figure 3: The structures of HLLCEP method, case 3: with only the right plastic wave.

The densities are

$$\rho_L^* = \frac{\rho_L(u_L - s_L)}{s^* - s_L}, \quad \rho_R^* = \frac{\widetilde{\rho}_R(\widetilde{u}_R - s_R)}{s^* - s_R}, \tag{3.76}$$

where the left and right elastic wave speeds are

$$s_L = \min(u_L - c_L, \widetilde{u}_R - \widetilde{c}_R), \quad s_R = \max(u_L + c_L, \widetilde{u}_R + \widetilde{c}_R). \tag{3.77}$$

The deviatoric stresses are

$$\overline{s}_{xxL}^* = -\frac{4}{3}\mu \ln(\frac{\rho_L^*}{\rho_L}) + s_{xxL}, \;\; \overline{s}_{xxR}^* = -\frac{4}{3}\mu \ln(\frac{\rho_R^*}{\rho_R}) + s_{xxR}, \tag{3.78}$$

$$s_{xxL}^* = \Upsilon(\overline{s}_{xxL}^*), \quad s_{xxR}^* = \Upsilon(\overline{s}_{xxR}^*). \tag{3.79}$$

The Cauchy stresses are

$$\sigma_L^* = \sigma_R^* = \sigma_L - \rho_L(s_L - u_L)(s^* - u_L), \tag{3.80}$$

and the pressures are

$$p_L^* = s_{xxL}^* - \sigma_L^*, \quad p_R^* = s_{xxR}^* - \sigma_R^*. \tag{3.81}$$

3.5.5 Case 4: with both the left and right plastic waves

If $|s_{xxL}| \leq \frac{2}{3}Y_0 \leq |\hat{s}_{xxL}^*|$ and $|s_{xxR}| \leq \frac{2}{3}Y_0 \leq |\hat{s}_{xxR}^*|$. Both the left side and right side exist plastic waves, as showed in Fig.4. The HLLCEP Riemann solver is given as

$$\boldsymbol{U}_{\text{Case4}}^{\text{HLLCEP}}(x,t) = \begin{cases} \boldsymbol{U}_L, & \text{if} \;\; \dfrac{x}{t} \leq s_L, \\ \boldsymbol{U}_L^*, & \text{if} \;\; s_L \leq \dfrac{x}{t} \leq \widetilde{s}_L, \\ \widetilde{\boldsymbol{U}}_L, & \text{if} \;\; \widetilde{s}_L \leq \dfrac{x}{t} \leq s^*, \\ \widetilde{\boldsymbol{U}}_R, & \text{if} \;\; s^* \leq \dfrac{x}{t} \leq \widetilde{s}_R, \\ \boldsymbol{U}_R^*, & \text{if} \;\; \widetilde{s}_R \leq \dfrac{x}{t} \leq s_R, \\ \boldsymbol{U}_R, & \text{if} \;\; \dfrac{x}{t} \geq s_R, \end{cases} \tag{3.82}$$

and the corresonding Eulerian and Lagrangian numerical flux are

$$\boldsymbol{F}^{\text{Euler}}_{\text{Case4}}(x,t)=\begin{cases}\boldsymbol{F}_L, & \text{if} \quad \dfrac{x}{t}\le s_L,\\ \boldsymbol{F}^*_L, & \text{if} \quad \widetilde{s}_L\le\dfrac{x}{t}\le s_L,\\ \widetilde{\boldsymbol{F}}_L, & \text{if} \quad s_L\le\dfrac{x}{t}\le s^*,\\ \widetilde{\boldsymbol{F}}_R, & \text{if} \quad s^*\le\dfrac{x}{t}\le s_R,\\ \boldsymbol{F}^*_R, & \text{if} \quad s_R\le\dfrac{x}{t}\le \widetilde{s}_R,\\ \boldsymbol{F}_R, & \text{if} \quad \dfrac{x}{t}\ge s_R,\end{cases} \tag{3.83}$$

$$\boldsymbol{F}^{\text{Lag}}_{\text{Case4}}(x,t)=\begin{cases}\widetilde{\boldsymbol{f}}_L, & \text{if} \quad s_*\ge\dfrac{x}{t},\\ \widetilde{\boldsymbol{f}}_R, & \text{if} \quad s^*\le\dfrac{x}{t}.\end{cases} \tag{3.84}$$

The states of $\widetilde{\boldsymbol{Q}}_L$ and $\widetilde{\boldsymbol{Q}}_R$ can be solved by the same process with Section 3.5.3 and Section 3.5.4. Then the states of $\boldsymbol{Q}^*_L$ and $\boldsymbol{Q}^*_R$ are given as following.

The speed of waves are evaluted as

$$s_L=\min(\widetilde{u}_L-\widetilde{c}_L,\widetilde{u}_R-\widetilde{c}_R),\quad s_R=\max(\widetilde{u}_L+\widetilde{c}_L,\widetilde{u}_R+\widetilde{c}_R), \tag{3.85}$$

$$s^*=\frac{\widetilde{\sigma}_L-\widetilde{\sigma}_R+\widetilde{\rho}_L\widetilde{u}_L(s_L-\widetilde{u}_L)-\widetilde{\rho}_R\widetilde{u}_R(s_R-\widetilde{u}_R)}{\widetilde{\rho}_L(s_L-\widetilde{u}_L)-\widetilde{\rho}_R(s_R-\widetilde{u}_R)}. \tag{3.86}$$

Then we can get the density using Eq.(3.76),

$$\rho^*_L=\frac{\widetilde{\rho}_L(\widetilde{u}_L-s_L)}{s^*-s_L},\quad \rho^*_R=\frac{\widetilde{\rho}_R(\widetilde{u}_R-s_R)}{s^*-s_R}, \tag{3.87}$$

and the deviatoric stresses are given as

$$\overline{s}^*_{xxL}=-\frac{4}{3}\mu\ln\left(\frac{\rho^*_L}{\rho_L}\right)+s_{xxL}, \tag{3.88}$$

$$\overline{s}^*_{xxR}=-\frac{4}{3}\mu\ln\left(\frac{\rho^*_R}{\rho_R}\right)+s_{xxR}, \tag{3.89}$$

$$\tag{3.90}$$

then using the von Mises' yielding condition,

$$s^*_{xxL}=\Upsilon(\overline{s}^*_{xxL}),\quad s^*_{xxR}=\Upsilon(\overline{s}^*_{xxR}). \tag{3.91}$$

The Cauchy stresses are solved as

$$\sigma^*_L=\sigma^*_R=\widetilde{\sigma}_L-\widetilde{\rho_L}(s_L-\widetilde{u}_L)(s^*-\widetilde{u}_L). \tag{3.92}$$

So we can get the pressure by $p=s_{xx}-\sigma$,

$$p^*_L=s^*_{xxL}-\sigma^*_L,\quad p^*_R=s^*_{xxR}-\sigma^*_R. \tag{3.93}$$

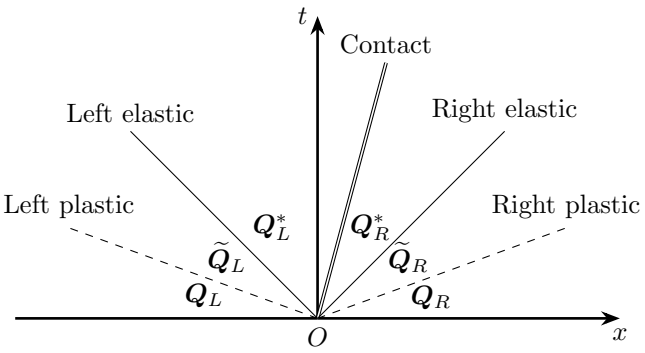

Figure 4: The structures of HLLCEP method, case 4: with both left and right plastic waves.

3.6 Summary of HLLCEP

Here, we present all the procedures of HLLCEP in a more simple way.

1. Assume there is no plastic wave in the Riemann solvers. Based on this assumption, we perform the following evaluations:

   (a) evaluate $\hat{s}^*$

   $$\hat{s}^* = \frac{\sigma_L - \sigma_R + \rho_L u_L(s_L - u_L) - \rho_R u_R(s_R - u_R)}{\rho_L(s_L - u_L) - \rho_R(s_R - u_R)}.$$

   (b) Evaluate $\hat{\rho}_L^*$ and $\hat{\rho}_R^*$

   $$\hat{\rho}_L^* = \frac{\rho_L(u_L - s_L)}{s^* - s_L}, \quad \hat{\rho}_R^* = \frac{\rho_R(u_R - s_R)}{s^* - s_R}.$$

   (c) Evaluate the deviatoric stress

   $$\hat{s}_{xxL}^* = -\frac{4}{3}\mu \ln(\frac{\hat{\rho}_L^*}{\rho_L}) + s_{xxL}, \;\; \hat{s}_{xxR}^* = -\frac{4}{3}\mu \ln(\frac{\hat{\rho}_R^*}{\rho_R}) + s_{xxR}.$$

   (d) Evaluate the pressure

2. Decide whether the state reach reach the elastic limit

   (a) If $|s_{xxL}| < \frac{2}{3}Y_0 \le |\hat{s}_{xxL}^*|$, left plastic wave exists, we need evaluate the left yielding state. The deviatoric stress, density and pressure behind the left plastic wave are given as

   $$\widetilde{s}_{xxL} = \begin{cases} -\dfrac{2}{3}Y_0, & \text{if} \quad \rho_L^* > \rho_L, \\ \dfrac{2}{3}Y_0, & \text{if} \quad \rho_L^* < \rho_L, \end{cases} \quad \widetilde{\rho}_L = \begin{cases} \rho_L \exp\left(\dfrac{Y_0}{2\mu} + \dfrac{3s_{xxL}}{4\mu}\right) & \text{if} \quad \rho_L^* > \rho_L, \\ \rho_L \exp\left(-\dfrac{Y_0}{2\mu} + \dfrac{3s_{xxL}}{4\mu}\right) & \text{if} \quad \rho_L^* < \rho_L, \end{cases}$$

   $$\widetilde{p}_L = \frac{2t(c_1 f(\widetilde{\rho}_L) + e_L) - (\sigma_L + \widetilde{s}_{xxL})}{2tc_0 - 1}, \quad t = \frac{\rho_L \widetilde{\rho}_L}{\widetilde{\rho}_L - \rho_L},$$

   and the Cauchy stress and velocity are

   $$\widetilde{\sigma}_L = -\widetilde{p}_L + \widetilde{s}_{xxL},$$

   $$\widetilde{u}_L = \begin{cases} u_L - \sqrt{\dfrac{\sigma_L - \widetilde{\sigma}_L}{t}} & \text{if} \;\; \rho_L^* > \rho_L, \\ u_L + \sqrt{\dfrac{\sigma_L - \widetilde{\sigma}_L}{t}} & \text{if} \;\; \rho_L^* < \rho_L. \end{cases}$$

   If left plactic wave does not exist,

   $$\widetilde{\boldsymbol{Q}}_L = \boldsymbol{Q}_L.$$

(b) If $|s_{xxR}| < \frac{2}{3}Y_0 \leq |\hat{s}^*_{xxR}|$, right plastic wave exists, , we need evaluate the right yielding state. The deviatoric stress, density and pressure behind the right plastic wave are given as

$$\widetilde{s}_{xxR} = \begin{cases} -\frac{2}{3}Y_0, & \text{if} \quad \rho^*_R > \rho_R, \\ \frac{2}{3}Y_0, & \text{if} \quad \rho^*_R < \rho_R, \end{cases} \quad \widetilde{\rho}_R = \begin{cases} \rho_R \text{exp}\left(\frac{Y_0}{2\mu} + \frac{3s_{xxR}}{4\mu}\right) & \text{if} \quad \rho^*_R > \rho_R, \\ \rho_R \text{exp}\left(-\frac{Y_0}{2\mu} + \frac{3s_{xxR}}{4\mu}\right) & \text{if} \quad \rho^*_R < \rho_R, \end{cases}$$

$$\widetilde{p}_R = \frac{2t(c_1 f(\widetilde{\rho}_R) + e_R) - (\sigma_R + \widetilde{s}_{xxR})}{2tc_0 - 1}, \quad t = \frac{\rho_R \widetilde{\rho}_R}{\widetilde{\rho}_R - \rho_R},$$

and the Cauchy stress and velocity are

$$\widetilde{\sigma}_R = -\widetilde{p}_R + \widetilde{s}_{xxR},$$

$$\widetilde{u}_R = \begin{cases} u_R + \sqrt{\frac{\sigma_R - \widetilde{\sigma}_R}{t}} & \text{if} \quad \rho^*_R > \rho_R, \\ u_R - \sqrt{\frac{\sigma_R - \widetilde{\sigma}_R}{t}} & \text{if} \quad \rho^*_R < \rho_R. \end{cases}$$

If right plactic wave does not exist,

$$\widetilde{\boldsymbol{Q}}_R = \boldsymbol{Q}_R.$$

3. re-evaluate the states in the star regions

(a) Solve the wave speeds,

$$s_L = \min(\widetilde{u}_L - \widetilde{c}_L, \widetilde{u}_R - \widetilde{c}_R), \quad s_R = \max(\widetilde{u}_L + \widetilde{c}_L, \widetilde{u}_R + \widetilde{c}_R),$$

$$s^* = \frac{\widetilde{\sigma}_L - \widetilde{\sigma}_R + \widetilde{\rho}_L \widetilde{u}_L (s_L - \widetilde{u}_L) - \widetilde{\rho}_R \widetilde{u}_R (s_R - \widetilde{u}_R)}{\widetilde{\rho}_L (s_L - \widetilde{u}_L) - \widetilde{\rho}_R (s_R - \widetilde{u}_R)}.$$

(b) Solve the densities,

$$\rho^*_L = \frac{\widetilde{\rho}_L (\widetilde{u}_L - s_L)}{s^* - s_L}, \quad \rho^*_R = \frac{\widetilde{\rho}_R (\widetilde{u}_R - s_R)}{s^* - s_R},$$

(c) Solve the deviatoric stresses,

$$\hat{s}^*_{xxL} = -\frac{4}{3}\mu \ln\left(\frac{\rho^*_L}{\widetilde{\rho}_L}\right) + \widetilde{s}_{xxL},$$
$$\hat{s}^*_{xxR} = -\frac{4}{3}\mu \ln\left(\frac{\rho^*_R}{\widetilde{\rho}_R}\right) + \widetilde{s}_{xxR},$$

then using the von Mises' yielding condition,

$$s^*_{xxL} = \Upsilon(\hat{s}^*_{xxL}), \quad s^*_{xxR} = \Upsilon(\hat{s}^*_{xxR}).$$

(d) Solving the Cauchy stresses,

$$\sigma^*_L = \sigma^*_R = \widetilde{\sigma}_L - \widetilde{\rho_L}(s_L - \widetilde{u}_L)(s^* - \widetilde{u}_L).$$

(e) The pressure is given by $p = s_{xx} - \sigma$.

4 A High-order cell-centered Lagrangian scheme for 1D conservative hydrodynamic equations with Wilkins' model

Here, we consider the following governing equations with Wilkins' model,

$$\begin{cases} \partial_t \rho + \partial_x(\rho u) = 0, \\ \partial_t(\rho u) + \partial_x(\rho u^2 + p - s_{xx}) = 0, \\ \partial_t(\rho E) + \partial_x([\rho E + p - s_{xx}]u) = 0, \\ \partial_t s_{xx} + u\partial_x s_{xx} - \dfrac{4}{3}\partial_x u = 0, \end{cases} \tag{4.1}$$

where $Q = (\rho, \rho u, \rho E, s_{xx})^T$. For a Lagrangian scheme, the governing equations also include the equation for moving the coordinates at the vertex of the mesh,

$$\frac{dx(t)}{dt} = u(x,t). \tag{4.2}$$

The spatial domain is discretized into N cells $I_i = [x_{i-1/2}, x_{i+1/2}]$ of space sizes $\Delta x_i = x_{i+1/2} - x_{i-1/2}$ for $i = 1, 2, \cdots, N$. For a given cell I_i, the cell center is denoted by x_i. The velocity $u_{i+1/2}$ is defined at the vertex of the mesh. The value of the cell average for the cell I_i is defined by

$$\overline{\boldsymbol{Q}}_i = \frac{1}{\Delta x_i}\int_{I_i} \boldsymbol{Q} dx. \tag{4.3}$$

4.1 Spatial discretization

The semi-discrete finite volume scheme of the conservative equations (4.1) in the cell I_i is written as

$$\frac{d(\overline{\boldsymbol{U}}_i \Delta x_i)}{dt} = -(\boldsymbol{F}_{i+\frac{1}{2}} - \boldsymbol{F}_{i-\frac{1}{2}}), \tag{4.4}$$

where

$$\boldsymbol{F}_{i+\frac{1}{2}} = \boldsymbol{\Phi}(\boldsymbol{Q}_{L,i+\frac{1}{2}}, \boldsymbol{Q}_{R,i+\frac{1}{2}}) = \begin{bmatrix} 0 \\ p_{i+\frac{1}{2}} - (s_{xx})_{i+\frac{1}{2}} \\ (p_{i+\frac{1}{2}} - (s_{xx})_{i+\frac{1}{2}})u_{i+\frac{1}{2}} \end{bmatrix}, \tag{4.5}$$

$\boldsymbol{Q}_{L,i+\frac{1}{2}}$ and $\boldsymbol{Q}_{R,i+\frac{1}{2}}$ represent the left and right values of $\boldsymbol{Q}$ at the cell's boundary $x_{i+\frac{1}{2}}$, and $p_{i+\frac{1}{2}}$, $(s_{xx})_{i+\frac{1}{2}}$ and $u_{i+\frac{1}{2}}$ denote the Godunov values at $x_{i+\frac{1}{2}}$, respectively.

The Godunov values $\boldsymbol{Q}_{i+\frac{1}{2}}$ can be solved by the Riemiann problem (3.1) at $x_{i+\frac{1}{2}}$,

$$\boldsymbol{Q}_{i+\frac{1}{2}} = \begin{cases} \boldsymbol{Q}_L^*, & \text{if } \dfrac{dx}{dt} \le s^*, \\ \boldsymbol{Q}_R^*, & \text{if } \dfrac{dx}{dt} > s^*, \end{cases} \tag{4.6}$$

where $\boldsymbol{Q}_L^*$, $\boldsymbol{Q}_R^*$ and s^* are evaluated by the HLLCEP in section 3.

Before this, we must give the left and right initial value ($\boldsymbol{Q}_{L,i+\frac{1}{2}}$ and $\boldsymbol{Q}_{R,i+\frac{1}{2}}$) by the cell average value $\overline{\boldsymbol{Q}}$ ($i = 1, 2, \cdots, N$). This process is done by the spatial reconstruction.

4.1.1 High-order reconstruction

The construction is carried out in the characteristic variables space in this paper, which is more stable and accurate than constructing $\boldsymbol{Q}_L$ and $\boldsymbol{Q}_R$ in the primative variables space or the conservative viables space.

First, we transform the conservative variables to local characteristic variables,

$$\boldsymbol{W} = \boldsymbol{L} \cdot \overline{\boldsymbol{Q}}, \tag{4.7}$$

where $\boldsymbol{L}$ is the left eigenvectors of $\boldsymbol{J}$, and $\boldsymbol{J}_i$ is the Jacobian matrix (3.3) in I_i.

Here, we use a third-order modified WENO scheme constructed in Ref.([13]) to reconstruct the characteristic variables at the left and right interfaces ($\boldsymbol{W}_L$ and $\boldsymbol{W}_R$) of every cell using $\boldsymbol{W}$. In the new Then projecting back to the consrvative variables space,

$$\boldsymbol{Q}_L = \boldsymbol{R} \cdot \boldsymbol{W}_L, \quad \boldsymbol{Q}_R = \boldsymbol{R} \cdot \boldsymbol{W}_R, \tag{4.8}$$

where $\boldsymbol{R}$ is the right eigenvectors of $\boldsymbol{J}$.

4.1.2 Spatial discretization of the constitutive equation

In the Lagrangian frame, the equation of the constitute model (2.8) can be written as

$$\frac{ds_{xx}}{dt} = \frac{4\mu}{3}\frac{\partial u}{\partial x}, \tag{4.9}$$

In order to satisfy the geometrical conservation, the volume of the cell I_i is evaluated by

$$V_i(t) = x_{i+\frac{1}{2}}(t) - x_{i-\frac{1}{2}}(t). \tag{4.10}$$

Taking the material derivative at both sides, we can get

$$\dot{V}_i(t) = \dot{x}_{i+\frac{1}{2}}(t) - \dot{x}_{i-\frac{1}{2}}(t), \tag{4.11}$$

as a result of (4.2), it becomes

$$\dot{V}_i(t) = u_{i+\frac{1}{2}}(t) - u_{i-\frac{1}{2}}(t), \tag{4.12}$$

combining (4.10), it becomes

$$\frac{\dot{V}_i(t)}{V_i} = \frac{u_{i+\frac{1}{2}}(t) - u_{i-\frac{1}{2}}(t)}{x_{i+\frac{1}{2}}(t) - x_{i-\frac{1}{2}}(t)}, \tag{4.13}$$

Using Eq.(2.7), we can get

$$\frac{\partial u}{\partial x} = \frac{u_{i+\frac{1}{2}}(t) - u_{i-\frac{1}{2}}(t)}{x_{i+\frac{1}{2}}(t) - x_{i-\frac{1}{2}}(t)}. \tag{4.14}$$

Then the discretization of the constitutive equation is given as

$$\frac{ds_{xx}}{dt} = \frac{4\mu}{3}\frac{u_{i+\frac{1}{2}}(t) - u_{i-\frac{1}{2}}(t)}{x_{i+\frac{1}{2}}(t) - x_{i-\frac{1}{2}}(t)}. \tag{4.15}$$

4.1.3 Reconstruction near the Multi-material interface

Using a high-order spatial scheme such as the third-order WENO scheme, the reconstruction across the interface may cause oscillation. So we need do some special treat near the interface. First, we track the interface by adding a marker function Mrk_i to mark the material in every cells. For two materials problem, we can initial Mrk as

$$\begin{cases} \mathrm{Mrk}(i) = 0, & \text{if cell } i \text{ is material A}, \\ \mathrm{Mrk}(i) = 1, & \text{if cell } i \text{ is material B}, \end{cases} \tag{4.16}$$

and we can get the interface is between cell ii and $ii+1$, if $\mathrm{Mrk}_{ii} = 0$ and $\mathrm{Mrk}_{ii+1} = 1$.

Using the reconstruction in the left side of the interface as an example. Constructing $\boldsymbol{W}_R(ii - \frac{1}{2})$ and $\boldsymbol{W}_L(ii + \frac{1}{2})$ are both with the stencil of $S^3 = (I_{ii-1}, I_{ii}, I_{ii+1})$, where cell I_{ii+1} is on the other side of the interface with a different EOS. Showed in Fig.5, we treat the interface as a special boundary and a ghost cell I'_{ii+1} is added on the right side to replace the use of I_{ii+1}.

The cell average values of the ghost cell I'_{ii+1} is given as follows, the Cauchy stress and the velocity are continuous across the interface according the relations in Eq.(3.18), so we use the real values on cell I_{ii+1}

$$\overline{\sigma}'_{ii+1} = \overline{\sigma}_{ii+1}, \quad \overline{u}'_{ii+1} = \overline{u}_{ii+1}. \tag{4.17}$$

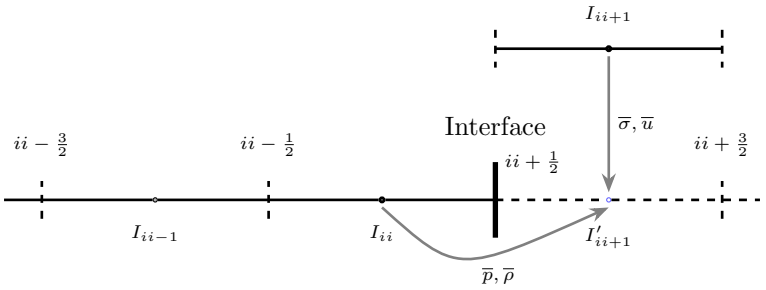

Figure 5: Ghost cell near the interface.

However, the values of pressure and density are not continuous, so we use a reflect condition on the interface as

$$\overline{p}'_{ii+1} = \overline{p}_{ii}, \quad \overline{\rho}'_{ii+1} = \overline{\rho}_{ii}. \tag{4.18}$$

After we get all the primative variables on the ghost cell I'_{ii+1}, using the EOS of material A on the left, we can get all the conservative variables $\boldsymbol{Q}'_{ii+1}$ and the characteristic variables $\boldsymbol{W}'_{ii+1}$ with the same process in Eq.(4.7). With the variables of $\boldsymbol{W}_{ii-1}$, $\boldsymbol{W}_{ii}$ and $\boldsymbol{W}'_{ii+1}$, we can reconstruct $\boldsymbol{W}_R(ii-\frac{1}{2})$ and $\boldsymbol{W}_L(ii+\frac{1}{2})$, respectively.

On the right side with the EOS of material B, setting a ghost cell of I'_{ii} in the stencil $S^3 = (I'_{ii}, I_{ii+1}, I_{ii+2})$ and using a samilar process, we can get new reconstructions of $\boldsymbol{W}_R(ii+\frac{1}{2})$ and $\boldsymbol{W}_L(ii+\frac{3}{2})$, respectively.

4.2 Time discretization

We use the third-order TVD-Runge-Kutta method as the time marching method, the TVD-Runge-Kutta method used in the Lagrangian schemes with von Mises' yielding condition is given in Ref.([12]) as follows.

Step 1,

$$\begin{aligned}
&x^{(1)}_{i+\frac{1}{2}} = x^{(0)}_{i+\frac{1}{2}} + \Delta t^n u^{(0)}_{i+\frac{1}{2}},\\
&\Delta x^{(1)}_i = x^{(1)}_{i+\frac{1}{2}} - x^{(1)}_{i-\frac{1}{2}},\\
&\Delta x^{(1)}_i \overline{\boldsymbol{U}}^{(1)}_i = \Delta x^{(0)}_i \overline{\boldsymbol{U}}^{(0)}_i + \Delta t^n \boldsymbol{L}(\overline{U}^{(0)}_i, (\overline{s_{xx}})^{(0)}_i, x^{(0)}_{i+\frac{1}{2}}),\\
&(\overline{\hat{s}_{xx}})^{(1)}_i = (\overline{s_{xx}})^{(0)}_i + \Delta t^n \Theta(u^{(0)}_{i+\frac{1}{2}}, x^{(0)}_{i+\frac{1}{2}}),\\
&(\overline{s_{xx}})^{(1)}_i = \Upsilon((\overline{\hat{s}_{xx}})^{(1)}_i).
\end{aligned} \tag{4.19}$$

Step 2,

$$\begin{aligned}
&x^{(2)}_{i+\frac{1}{2}} = \frac{3}{4} x^{(0)}_{i+\frac{1}{2}} + \frac{1}{4}\left(x^{(1)}_{i+\frac{1}{2}} + \Delta t^n u^{(1)}_{i+\frac{1}{2}}\right),\\
&\Delta x^{(2)}_i = x^{(2)}_{i+\frac{1}{2}} - x^{(2)}_{i-\frac{1}{2}},\\
&\Delta x^{(2)}_i \overline{\boldsymbol{U}}^{(2)}_i = \frac{3}{4}\Delta x^{(0)}_i \overline{\boldsymbol{U}}^{(0)}_i + \frac{1}{4}\left(\Delta x^{(1)}_i \overline{\boldsymbol{U}}^{(1)}_i + \Delta t^n \boldsymbol{L}(\overline{U}^{(1)}_i, (\overline{s_{xx}})^{(1)}_i, x^{(1)}_{i+\frac{1}{2}}\right),\\
&(\overline{\hat{s}_{xx}})^{(2)}_i = \frac{3}{4}(\overline{s_{xx}})^{(0)}_i + \frac{1}{4}\left((\overline{s_{xx}})^{(1)}_i + \Delta t^n \Theta(u^{(1)}_{i+\frac{1}{2}}, x^{(1)}_{i+\frac{1}{2}})\right),\\
&(\overline{s_{xx}})^{(2)}_i = \Upsilon((\overline{\hat{s}_{xx}})^{(2)}_i).
\end{aligned} \tag{4.20}$$

Step 3,

$$
\begin{aligned}
&x_{i+\frac{1}{2}}^{(3)} = \frac{1}{3}x_{i+\frac{1}{2}}^{(0)} + \frac{2}{3}\left(x_{i+\frac{1}{2}}^{(2)} + \Delta t^n u_{i+\frac{1}{2}}^{(2)}\right),\\
&\Delta x_i^{(3)} = x_{i+\frac{1}{3}}^{(2)} - x_{i-\frac{1}{2}}^{(3)},\\
&\Delta x_i^{(3)}\overline{\boldsymbol{U}}_i^{(2)} = \frac{1}{3}\Delta x_i^{(0)}\overline{\boldsymbol{U}}_i^{(0)} + \frac{2}{3}\left(\Delta x_i^{(1)}\overline{\boldsymbol{U}}_i^{(2)} + \Delta t^n \boldsymbol{L}(\overline{U}_i^{(2)}, (\overline{s_{xx}})_i^{(2)}, x_{i+\frac{1}{2}}^{(2)}\right),\\
&(\overline{\hat{s}_{xx}})_i^{(3)} = \frac{1}{3}(\overline{s_{xx}})_i^{(0)} + \frac{2}{3}\left((\overline{s_{xx}})_i^{(2)} + \Delta t^n \Theta(u_{i+\frac{1}{2}}^{(2)}, x_{i+\frac{1}{2}}^{(2)})\right),\\
&(\overline{s_{xx}})_i^{(3)} = \Upsilon((\overline{\hat{s}_{xx}})_i^{(3)}).
\end{aligned}
\tag{4.21}
$$

Where $\boldsymbol{L}$ and Θ are the numerical spatial operators representing the right hands of Eq.(4.4) and Eq.(4.15), respectively, and the variables with the superscripts n and $n+1$ denote the values of the corresponding variables at the n-th and $(n+1)$-th time steps, respectively.

5 Numerical tests

In this section, the new HLLCEP method is tested in different problems to see the capibility of capturing elastic-plastic waves, espicially in the problem with different materials interface.

5.1 Accuracy test

In the first test, a smooth solution is used to test the accuracy of the scheme. The computational domian is $[0, 1]$, and a periodic boundary condition is used. The EOS is given by the Mie-Grüneisen model with the parameters $\rho_0 = 8930\text{kg/m}^3$, $a_0 = 3940\text{m/s}$, $\Gamma_0 = 2$, and $s = 1.49$. The constitutive model has the parameters, $\mu = 4.5 \times 10^10\text{Pa}$ and $Y^0 = 9 \times 10^10\text{Pa}$. The initial condition is given as

$$
\rho = \rho_0(1 - b\sin(2\pi x)), \quad u = a, \quad p = 1.1\rho u^2, \quad s_{xx} = s_0\sin(2\pi x), \tag{5.1}
$$

where $a = 10,000\text{m/s}$, $b = 0.1$ and $s_0 = 6 \times 10^5\text{Pa}$.

The final results are given at time $t = 1 \times 10^{-4}$. The reference result is computed with a refined mesh of $N = 2000$, the L_1- and L_∞-norm errors are showed in Table 5.1. We can see that, with a modified third-order WENO scheme, the high-order cell-centered Lagrangian scheme can achieve the designed accuracy.

Table 5.1: The accuracy with smooth solution.

	N	L_1 error	L_1 order	L_∞ error	L_∞ order
ρ	50	7.74×10^{-5}	—	3.34×10^{-4}	—
	100	9.84×10^{-6}	2.97	3.47×10^{-5}	3.27
	200	1.40×10^{-6}	2.81	6.85×10^{-6}	2.34
	400	2.25×10^{-7}	2.63	1.33×10^{-6}	2.36
s_{xx}	50	8.21×10^{-4}	—	3.55×10^{-3}	—
	100	1.04×10^{-4}	2.98	3.68×10^{-4}	3.27
	200	1.48×10^{-5}	2.81	7.27×10^{-5}	2.33
	400	2.39×10^{-6}	2.63	1.42×10^{-4}	2.36

5.2 Piston problem

In the second test, we consider the piston problem [14] with a piece of copper with the initial condition of

$$
\rho = 8930\text{kg/m}^3, \quad p = 10^5\text{Pa}, \quad u = 0\text{m/s}, \quad s_{xx} = 0\text{Pa}. \tag{5.2}
$$

The EOS for copper is given by the Mie-Grüneisen model with the parameters

$$
\rho_0 = 8930\text{kg/m}^3, \quad a_0 = 3940\text{m/s}, \quad ,\Gamma_0 = 2, \quad s = 1.49. \tag{5.3}
$$

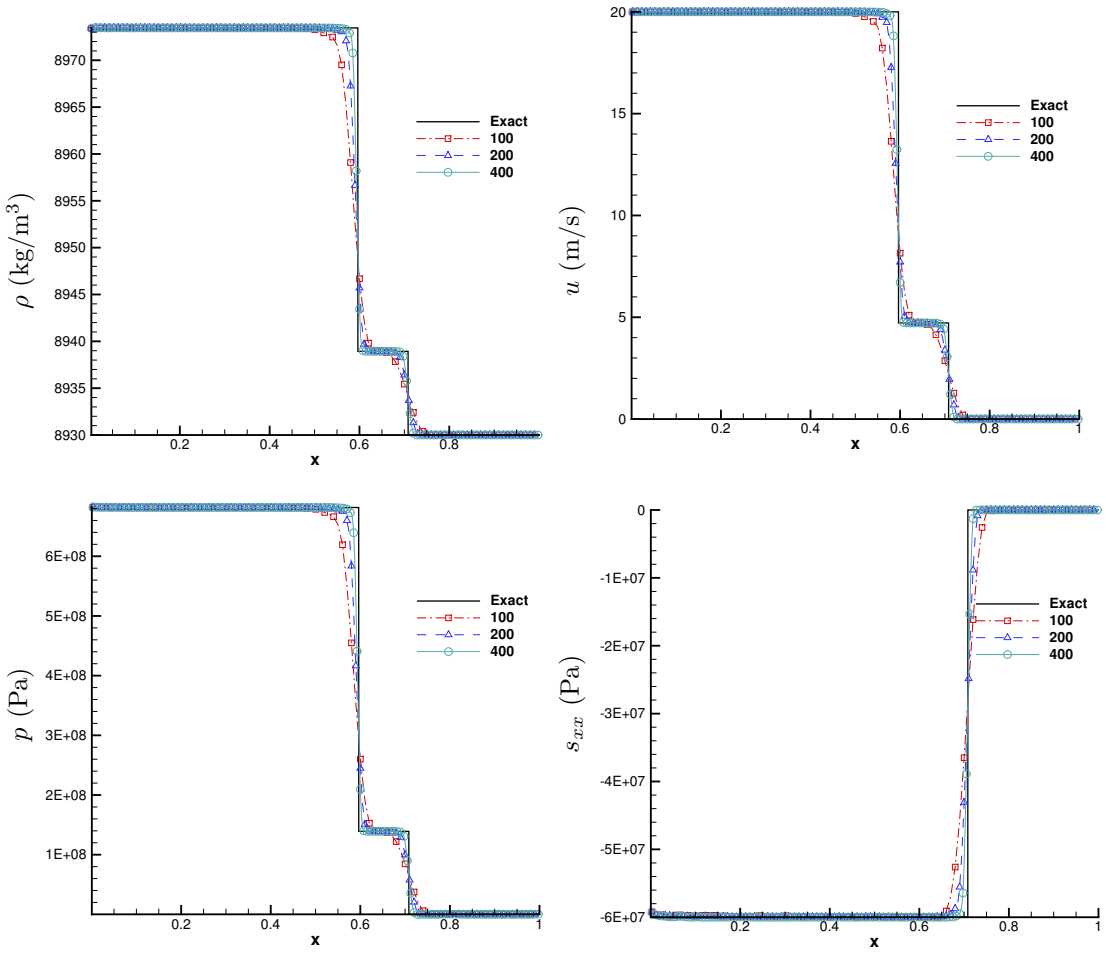

Figure 6: The result of Piston problem

The constitutive model is characterized by the following parameters,

$$\mu = 4.5 \times 10^{10}\text{Pa}, \quad Y_0 = 9 \times 10^{7}\text{Pa}. \tag{5.4}$$

The left boundary condtion is a velocity boundary condition with $u_{\text{piston}} = 20\text{m/s}$, and the right boundary is a wall boundary condition.

In Fig.6, we test the convergence of the scheme with different meshes of 100, 200 and 400 cells. The final time is $t = 150\mu s$. We can see that the current scheme can capture the leading elastic shock wave and the followed plastic wave well without oscillation.

5.3 Wilkins' problem

This problem, first introduced by Wilkins, is used to test the ability of capturing rarefaction waves of scheme. In this problem, a moving alumimium plate striking on another alumimium plate. The EOS for aluminium is given by the Mie-Grüneisen model with the parameters $\rho_0 = 2785\text{kg/m}^3$, $a_0 = 5328\text{m/s}$, $\Gamma_0 = 2$ and $s = 1.338$. The constitutive model is characterized by the parameters $\mu = 2.76 \times 10^{10}\text{Pa}$ and $Y_0 = 3 \times 10^{8}\text{Pa}$. The initial condtions are given as

$$\begin{cases} \rho = 2785\text{kg/m}^3, \quad u = 800\text{m/s}, \quad p = 10^{-6}\text{Pa}, \quad \text{if} \quad 0\text{m} \le x \le 5 \times 10^{-3}\text{m}, \\ \rho = 2785\text{kg/m}^3, \quad u = 0\text{m/s}, \quad p = 10^{-6}\text{Pa}, \quad \text{if} \quad 5 \times 10^{-3}\text{m} \le x \le 50 \times 10^{-3}\text{m}. \end{cases} \tag{5.5}$$

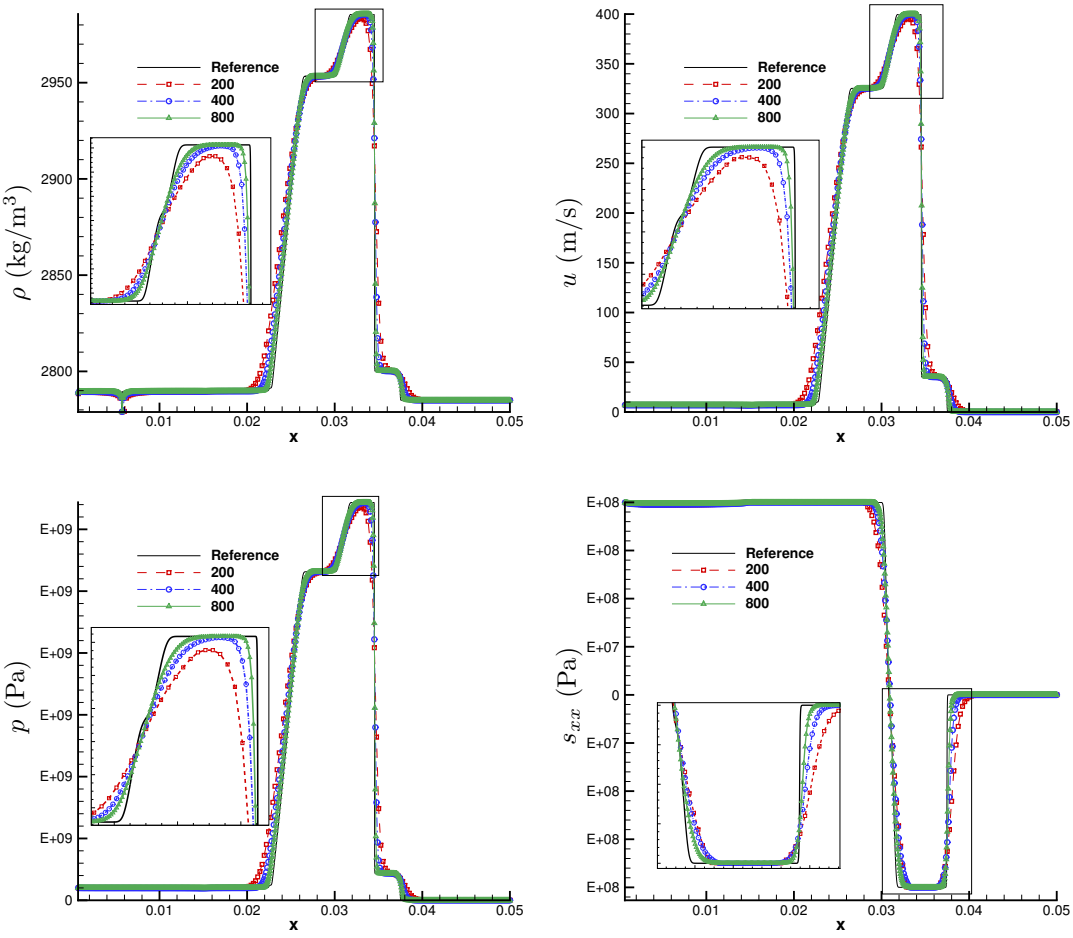

Figure 7: The result of Wilkins problem

The left boundary is set as free boundary and on the right we use a wall boundary condtion. The final time is $t = 5 \times 10^{-6}$s. In Fig.7, we give the results simulated with 200, 400 and 800 cells, the reference result is given by a refined mesh with 4000 cells. Showed in the figures and these locally enlarged plots, the elastic and plastic right-going shocks and the reflected elastic and plastic rarefaction waves are well resloved without oscillation.

5.4 Multi-material problem 1

Then we consider a multi-material problem without the plasticity effect. A similar case is used in Ref.([15]). In this test, a moving copper stricks on an aluminium plate. The parameters for the EOSs and constitutive model for aluminum and copper are $(\rho_0, a_0, \Gamma_0, s, \mu)_{\text{Al}} = (8930\text{kg/m}^3, 3940\text{m/s}, 2, 1.49, 2.76, 2.76 \times 10^{10}\text{Pa})$ and $(\rho_0, a_0, \Gamma_0, s, \mu)_{\text{Cu}} = (2785\text{kg/m}^3, 5328\text{m/s}, 2, 1.338, 4.5 \times 10^{10}\text{Pa})$, respectively. In order to remove the influence of the plasticity effect, we use a very large unphysics yield strength $Y_0 = 3 \times 10^{12}$Pa. The initial conditions of this problem are

$$\begin{cases} \rho = 2785\text{kg/m}^3, \quad u = u_0, \quad p = 10^{-12}\text{Pa}, s_{xx} = 0, \quad \text{if } \ 0\text{m} \le x \le 2.5 \times 10^{-2}\text{m}, \\ \rho = 8930\text{kg/m}^3, \quad u = 0\text{m/s}, \quad p = 10^{-12}\text{Pa}, s_{xx} = 0, \quad \text{if } \ 2.5 \times 10^{-2}\text{m} \le x \le 50 \times 10^{-2}\text{m}. \end{cases} \tag{5.6}$$

In this case we take $u_0 = 100$m/s. Figure 8 shows the numerical results computed by HLLCE and HLLCEP at the final time $t = 2 \times 10^{-6}s$, the reference is given by a refined mesh with 4000 cells. We can see there is

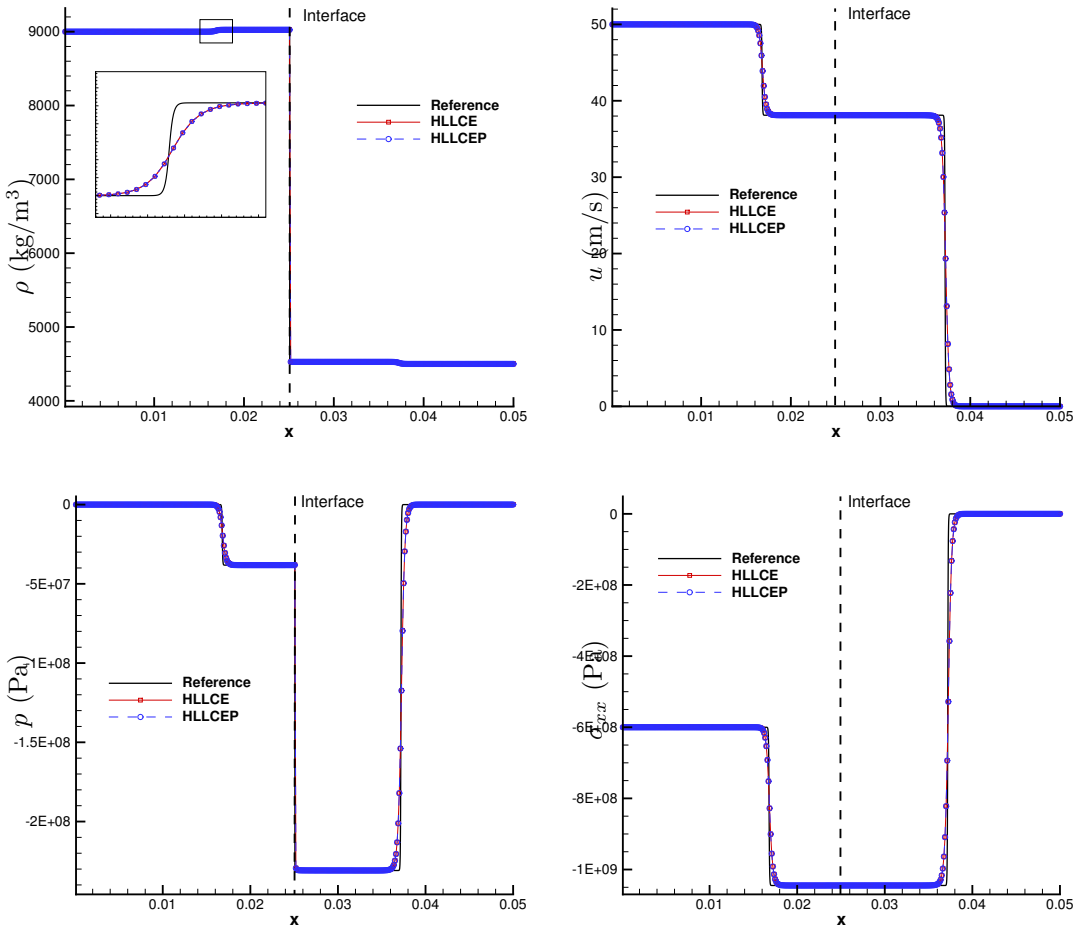

Figure 8: The result of two-materials problem 1

little difference between the two schemes in the multi-material case without plastic wave.

5.5 Two materials problem 2

Next, we consider a similar problem but with plasticity effect. The yield strengths are $Y_0^{\mathrm{Cu}} = 9 \times 10^7$ and $Y_0^{\mathrm{Al}} = 3 \times 10^8$, respectively. All other parameters are same to those in problem 5.4. The inital condition is also same as Eq.(5.6), we consider this case with a velocity of $u_0 = 60$m/s. Fig.9 gives the result at final time $t = 2 \times 10^{-6}$s with 200 cell, the solution computed by the HLLCE scheme is taken as a comparasion. The reference solution is given by a refine mesh with 4000 cells. We can see that using HLLCE, the Cauchy stress is not constitutive across the interface, this does not confirm with the relation of Eq.(3.18), while with the new HLLCEP scheme, we can get a correct and stable result.

Conclutions

In this paper, a new HLLC-type approximate Reimann solver is constructed to simulate 1D multi-material elastic-plastic flows with the hypo-elastic constitutive model and the von Mises yield criterion. For the elastic-plastic problems with multi-materials, the relations between the interface is difficult to satisfied. Within a detail consideration of the plastic waves, there is no unreasonable assumption, such as the continuous pressure

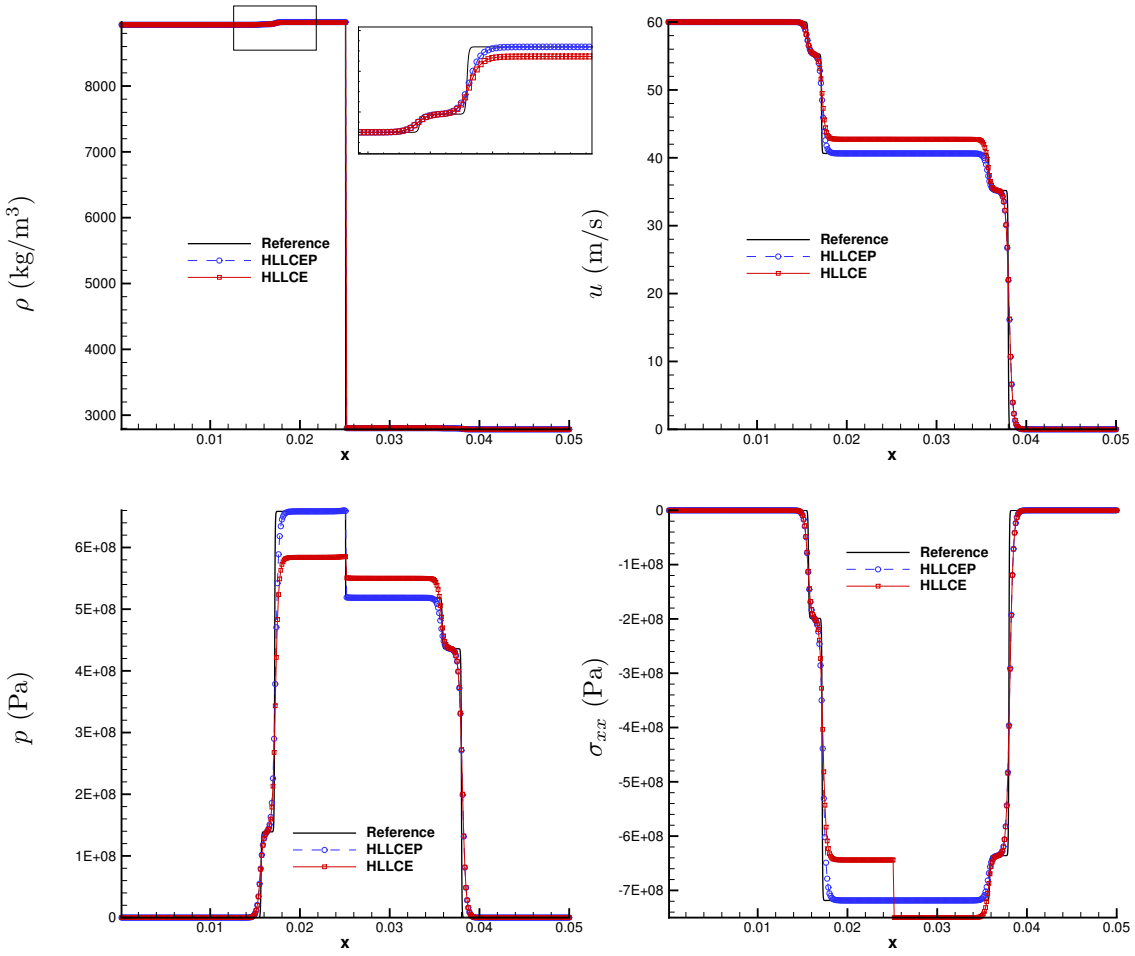

Figure 9: The result of two-materials problem 2

assumption between the interface, is used in the new HLLCEP method. And thus, the new method can resolve all the wave structures in multi-material elastic-plasitc problems with accuracy and stability.

Acknowledgement

References

[1] M. L. Wilkins, Calculation of elastic-plastic flow, Tech. rep., California Univ Livermore Radiation Lab (1963).

[2] J. A. Trangenstein, P. Colella, A higher-order godunov method for modeling finite deformation in elastic-plastic solids, Communications on Pure and Applied mathematics 44 (1) (1991) 41–100.

[3] G. Miller, P. Colella, A high-order eulerian godunov method for elastic–plastic flow in solids, Journal of computational physics 167 (1) (2001) 131–176.

[4] P. T. Barton, D. Drikakis, E. Romenski, V. A. Titarev, Exact and approximate solutions of riemann problems in non-linear elasticity, Journal of Computational Physics 228 (18) (2009) 7046–7068.

[5] D. Burton, T. Carney, N. Morgan, S. Sambasivan, M. Shashkov, A cell-centered lagrangian godunov-like method for solid dynamics, Computers & Fluids 83 (2013) 33–47.

[6] G. Kluth, B. Després, Discretization of hyperelasticity on unstructured mesh with a cell-centered lagrangian scheme, Journal of Computational Physics 229 (24) (2010) 9092–9118.

[7] P.-H. Maire, R. Abgrall, J. Breil, R. LoubèRe, B. Rebourcet, A nominally second-order cell-centered lagrangian scheme for simulating elastic–plastic flows on two-dimensional unstructured grids, Journal of Computational Physics 235 (2013) 626–665.

[8] J.-B. Cheng, W. Huang, S. Jiang, B. Tian, A third-order moving mesh cell-centered scheme for one-dimensional elastic-plastic flows, Journal of Computational Physics 349 (2017) 137–153.

[9] S. L. Gavrilyuk, N. Favrie, R. Saurel, Modelling wave dynamics of compressible elastic materials, Journal of computational physics 227 (5) (2008) 2941–2969.

[10] B. Despres, A geometrical approach to nonconservative shocks and elastoplastic shocks, Archive for Rational Mechanics and Analysis 186 (2) (2007) 275–308.

[11] J.-B. Cheng, E. F. Toro, S. Jiang, M. Yu, W. Tang, A high-order cell-centered lagrangian scheme for one-dimensional elastic–plastic problems, Computers & Fluids 122 (2015) 136–152.

[12] J. Cheng, Harten-lax-van leer-contact (hllc) approximation riemann solver with elastic waves for one-dimensional elastic-plastic problems, Applied Mathematics and Mechanics 37 (11) (2016) 1517–1538.

[13] S. Liu, Y. Shen, B. Chen, F. Zeng, Novel local smoothness indicators for improving the third-order weno scheme, International Journal for Numerical Methods in Fluids 87 (2) (2018) 51–69.

[14] P.-H. Maire, R. Abgrall, J. Breil, J. Ovadia, A cell-centered lagrangian scheme for two-dimensional compressible flow problems, SIAM Journal on Scientific Computing 29 (4) (2007) 1781–1824.

[15] N. S. Ghaisas, A. Subramaniam, S. K. Lele, High-order eulerian methods for elastic-plastic flow in solids and coupling with fluid flows, in: 46th AIAA Fluid Dynamics Conference, 2016, p. 3350.